ISSN (Print) 1226-1750
ISSN (Online) 2233-6656
Journal of Magnetics 26(1), 60-66 (2021) https://doi.org/10.4283/JMAG.2021.26.1.060

Design Optimization for Pullout Torque Improvement of a Magnetic Coupling in Chemical Pump Application

Se-Hyun Rhyu[1], Sunil Kumar[1]*, Salman Khaliq[1], Myung-Hwan Yoon[1], Jeong-Eui Yun[2], and Sang-Seon Lee[3]

[1]*Intelligent Mechatronics Research Center, Korea Electronics Technology Institute (KETI), Republic of Korea*
[2]*School of Mechanical System Engineering, Kangwon National University, Republic of Korea*
[3]*President & Chief Executive Officer (CEO), Fluonics Co., Ltd, Republic of Korea*

(Received 7 August 2020, Received in final form 26 January 2021, Accepted 3 February 2021)

This paper presents magnet shape optimization of permanent magnet coupling (PMC) for a 50 hp chemical pump system considering the linear and non-linear design parameters. Firstly, the size and topology of PMC are considered for the initial model. PM eddy currents are analyzed to select the initial model. Secondly, an optimization process is performed to get the maximum pullout torque for a given PM volume. The optimization is based on a two step process; firstly, non-linear design parameters are considered for optimization using 2-D finite element method (FEM). The optimization is performed to maximize the pullout torque of the PMC and reducing the PM volume. Kriging method and genetic algorithm are utilized due to the non-linearity of the design parameters in the optimization process. Secondly, linear design parameters are adjusted and 3-D FEM is utilized to achieve the target and incorporate the end effects. Using two-step design process, the number of design parameters are reduced in the first step which simplify the optimization process and computational time is reduced using 2-D FEM. After that, the axial length of the PMC can be used as a linear design parameter to obtain the required pull-out torque. The optimized model is then simulated using 3-D FEM to incorporate the end effects and experimental results are then presented.

Keywords : finite element method (FEM), genetic algorithm (GA), and permanent magnet coupling (PMC)

1. Introduction

Mechanical couplings and gears need a mechanical contact resulting in noise, dust ingression, and maintenance of the system. On the other hand, permanent magnet couplings (PMC) have been used for complete isolation or hermetic seal of the load from the driving motor preventing the passage of air, oil, or any fluid mixture [1], [2]. They are also utilized as torque limiter in certain applications in order to avoid transmitting torque overloads [3].

Several types of PMCs have been investigated depending on number of poles and PM span [1-6]. Usually, there are multiple number of poles and a shorter PM span is considered for the design depending on the size of the PMC. However, the leakage flux due to multiple number of poles and PM span increases with respect to the increasing airgap between the inner and outer rotating parts [4]. This condition becomes significant while designing a large size and high power PMC since the amount PM volume and cost increases considerably. As pullout torque is generally considered 2-to-4 times the rated torque of the system, proper utilization of the PMs should be carefully investigated in designing a large scale PMC to achieve highest possible pullout torque. A 15 hp PMC has been already designed and optimized for maximum pullout torque per PM volume using PM dimensions as design parameters [6]. For a larger PMC, such as 50 hp, it is highly recommended to further optimize the PM shape in order to further reduce the overall cost of the PMs (NdFeB and SmCo). A different approach is considered in this paper for the design process and optimization.

In this paper, a 12-pole PMC is presented for a 50 hp chemical fluid pump system. The system's rated torque is 103.2 Nm with a rated speed of 3,450 RPM, while the PMC is designed to have a pull-out torque of four times

©The Korean Magnetics Society. All rights reserved.
*Corresponding author: Tel: +82-32-621-2870
Fax: +82-32-621-2855, e-mail: sunilkumarbachani@gmail.com

© 2021 Journal of Magnetics

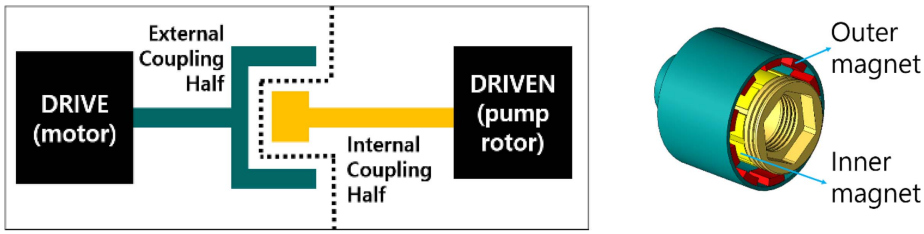

(a) (b)

Fig. 1. (Color online) Magnetic Coupling. (a) Concept, (b) 3-D Schematic.

the rated torque of the system, i.e., 413 Nm. Surface type PMs are utilized and the PM shape is optimized to yield maximum pullout torque. Fig. 1 shows the structure of a radial-flux type PMC. Primary shaft mover is connected with the driving motor while the secondary follower shaft is connected to the pump load. The inner part of the PMC which comes in contact with the chemical fluid are coated with a layer of Teflon lining in order to avoid the reaction of the chemical fluid.

2. Proposed Design and Optimization

There are two parts of a PMC; driver or outer part, which is connected to the driving motor and follower or inner part, which is connected to the chemical pump load. The detailed PMC design specifications are listed in Table 1. The PM material is selected considering the operating temperature of the inner and outer parts of the PMC. The inner part of the PMC is covered with Teflon lining to protect the PMs from the high temperature chemical fluid. The fluid temperature is estimated to be 170 ºC and therefore, Samarium Cobalt (SmCo) PMs are used for the inner part of the PMC. SmCo are selected due to their ability to withstand higher temperatures without demagnetizing. However, the outer part of the PMC is not susceptible to much higher temperatures and therefore, NdFeB PMs are utilized due to relatively lower cost. Generally, the price of SmCo PMs are considered twice than that of NdFeB.

There needs to be a large separation between the driver and the follower to incorporate the pump containment or shell. The containment shell thickness is 5 mm. The inner part PMs are covered with 4.5 mm length of the Teflon lining in to order to protect the PMs from the chemical fluid. The physical separation of the inner part from the containment shell is 1.5 mm whereas the separation of outer part from the containment shell is 2.0 mm. This results in overall gap between the outer and inner PMs of 13 mm.

Firstly, two models are designed considering starting

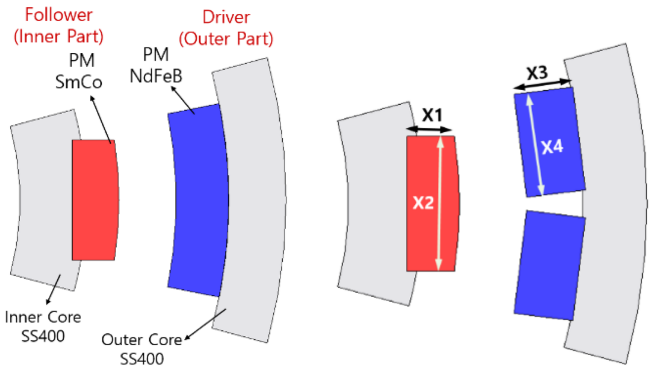

(a) (b)

Fig. 2. (Color online) Proposed 12-pole PMC 1/12th model. (a) Model-1 description, (b) Model-2 optimization parameters.

eddy currents in the PMs as shown in Fig. 2. Model-1 is based on conventional ring type PM on the outer part of the PMC. Model-2 is based on a two-piece PM-pole with rectangular PMs. The PM design variables are selected based on the thickness and width of the PMs as shown in Fig. 2(b). The reason for using two-piece PM-pole is to analyze the effect of starting eddy current. Based on the eddy current analysis, the selected model is then optimized using suitable design parameters to get the maximum pullout torque and minimum PM volume.

Table 1. PMC Dimension Specifications and Operating Conditions.

Item	Unit	Value
Outer diameter	mm	251
Outer part inner diameter	mm	201
Inner part outer diameter	mm	175
Separation length	mm	13
Number of poles	–	12
Rated angular speed	RPM	3,450
Maximum Fluid Temperature	ºC	170
System Output Power	hp	50
Target Pullout Torque	Nm	413

2.1. Eddy Current Analysis

Starting a high power PMC generally requires a large pullout torque. The eddy currents in the PMs are generated due to rotor speed difference or slip of the inner and outer parts at the starting of the PMC. The large eddy currents generate heat in the PMs and thereby reducing the magnetic strength of the PMs. The reduced magnetic strength will decrease the pullout torque of the PMC which may cause trouble in starting the PMC. Therefore, eddy current analysis is performed to verify the effectiveness of the investigated models in terms of eddy current heat loss.

Two models have been investigated as shown in Fig. 2. Model-1 is based on conventional one-piece pole NdFeB PM whereas Model-2 is based on rectangular two-piece pole configuration. The eddy currents generated in PM pole will be reduced by splitting PM pole in two or more pieces. It is for this reason, the PMs in the outer part of the PMC are split into two-pieces. Since the outer part contains a relatively larger PM span, this makes enough room to split the outer PMs into two rectangular pieces. This configuration will reduce the eddy currents at the starting of the PMC. The PMs on the inner part of the PMC are kept as whole due to manufacturing constraints.

FEM analysis is carried out to investigate the amount of eddy currents in both the models. The volume of PM pole in both Model-1 and Model-2 is kept the same for the analysis and comparison. The eddy currents in the PMs are generated by applying some amount of slip between the inner and outer rotating parts. The slip is defined as the difference in rotational speed between the inner and outer parts of the PMC. The value of slip is kept same in both the models for fair comparison. The value of eddy currents is different at various time instants; therefore, a specific time instant is considered to compare the eddy current density of the models. Fig. 3 shows the eddy current density plot of the outer PM pole of both the models. It can be seen that the amount of eddy currents has been considerably reduced in case of Model-2 as compared to Model-1, as expected. The maximum eddy current density in case of Model-1 is found to be 41.7 mA/mm^2 while in case of Model-2, it is reduced to 21.9 mA/mm^2. Hence, Model-2 can perform better in terms of starting eddy current loss compared to Model-1. Therefore, Model-2 is selected for further analysis and optimization.

2.2. Optimization

The effect of PM thickness and PM Span is non-linear on the output pullout torque. Therefore, only non-linear parameters are selected for the optimization in order to effectively optimize the design as shown in Fig. 2(b). The detailed design and optimization process flow is shown in Fig. 4. This optimization process has been utilized in [6] due to non-linear design parameters. The follower outer diameter and the driver inner diameter are kept fixed throughout the optimization process and the PM thicknesses are varied according to design of experiments (DOE). Since there can be many design parameters for the optimization, only non-linear design parameters are selected. This allows the optimization results to deal with non-linearity effectively and reduce complexity which results from two much design parameters. Latin Hypercube Sampling (LHS) method is considered to generate samples for DOE. These samples are then simulated using 2-D FEM to get the pullout torque and the PM volume is calculated. The pullout torque per PM volume is then calculated. 2-D FEM is used at this stage to reduce the computation time. The outer core thickness can be adjusted according to the outer PM thickness in each sample model in order to allow sufficient amount of flux without

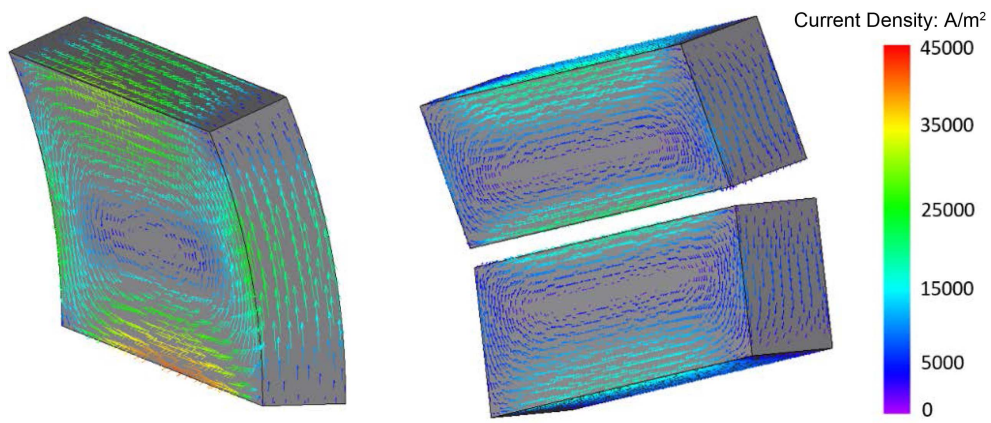

(a) (b)

Fig. 3. Eddy Current Density in NdFeB PM. (a) Model-1 (b) Model-2.

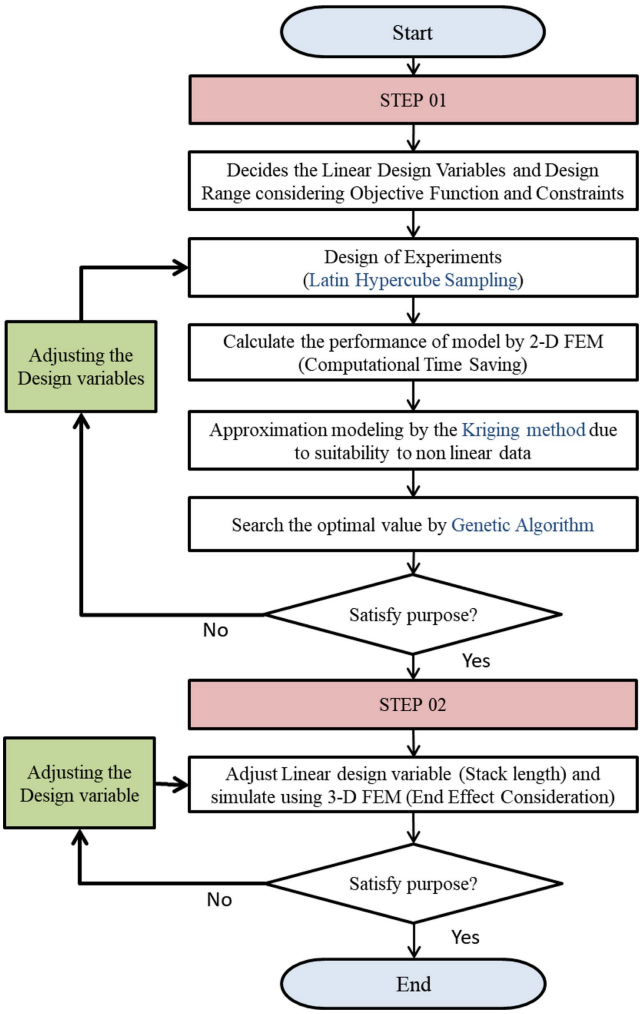

Fig. 4. (Color online) Design and Optimization process.

saturation. Stack length, being linear function of the pull-out torque, is kept constant as 100 mm in all the samples. After that, Kriging method is utilized along with genetic algorithm to get the optimized result due to their effectiveness in analyzing non-linear design parameters. The objective functions, design variables, constraints, and optimized design parameters are shown below.

- <u>Objective:</u>
  Maximize Pullout Torque
  Minimize PM Volume
- <u>Design variables and range</u>:
  $8.0 \leq X1 \leq 11.5$ mm
  $18 \leq X2 \leq 26$ degrees
  $09 \leq X3 \leq 15$ mm
  $12 \leq X4 \leq 24$ mm
- <u>Optimized design variables:</u>
  X1 = 09.71 mm

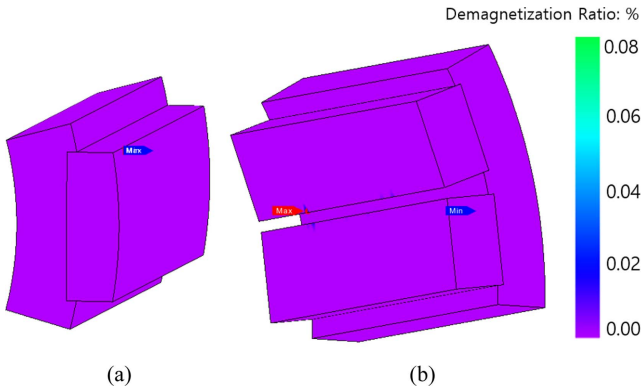

Fig. 5. (Color online) Demagnetization ratio plot. (a) Inner part, (b) Outer part.

X2 = 19.74 deg
X3 = 13.04 mm
X4 = 21.89 mm

3. FEM Results and Analysis

The optimized model is selected using above mentioned optimization process is found to have highest value of pullout torque per PM volume. The optimized design variables are then verified using 2-D FEM. The pullout torque/PM volume of the optimized model is calculated as 372.2 Nm/dm^3. The initial benchmark model was found to have a pullout torque/PM volume of 366.5 Nm/dm^3. Hence, the optimized model has improved performance in terms of pullout torque/PM volume.

After that, the optimized model is 3-D simulated by adjusting the stack length to get the target pull-out torque and considering the end effects. The final model is found to have a stack length of 102 mm with a pullout torque of 418 Nm. The magnetic flux density plot of the optimized model is shown in Fig. 6. The magnetic flux density in

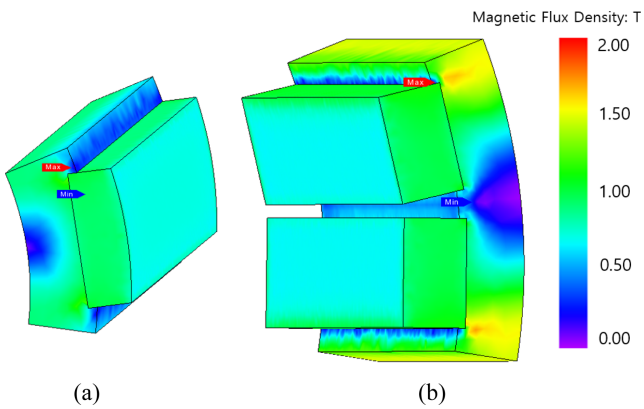

Fig. 6. (Color online) Optimized 1/12th Model - Magnetic Flux Density Plot. (a) Inner part, (b) Outer part.

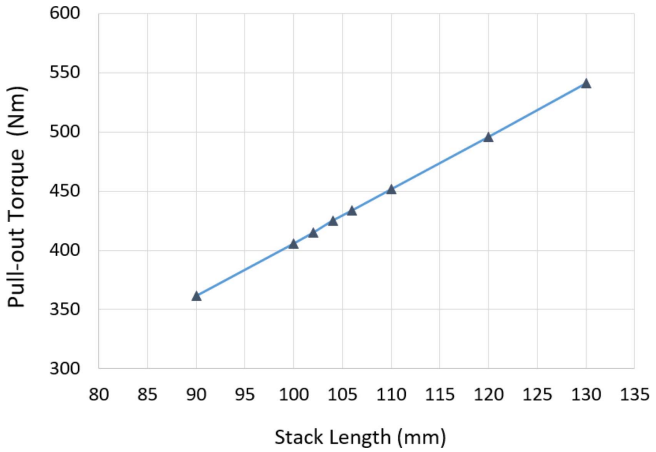

Fig. 7. (Color online) Pullout torque variation with stack length.

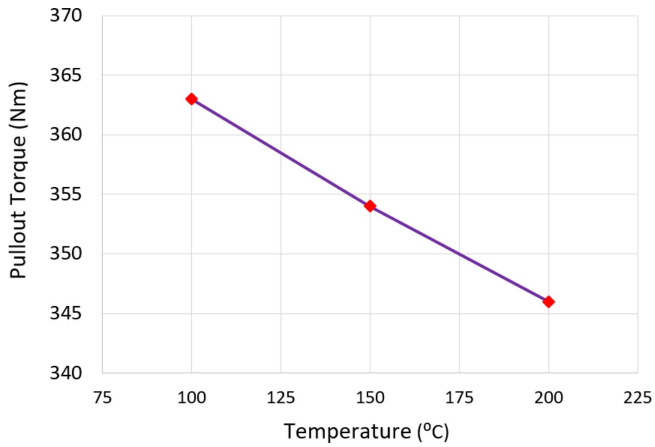

Fig. 8. (Color online) Pullout torque variation with PM temperature.

the iron core is within the saturation limits. The stack length of the optimized model is adjusted to get the target pullout torque of 413 Nm. Fig. 7 shows the variation of pullout torque with respected to stack length of the optimized model. This variation is found to be linear as expected. 3-D FEM is utilized in order to select the final stack length of 102 mm which results in a pullout torque of 415 Nm.

Furthermore, temperature analysis is also performed to analyze the effect of PM temperature on pullout torque. The SmCo PM is subject to higher temperature of up to 170 °C whereas the NdFeB PM is not in contact with any heat source of hot fluid. The analysis is carried by fixing NdFeB temperature to 100 °C and the temperature of SmCo PM is varied up to 200 °C. The pullout torque variation with respect to SmCo PM temperature is shown in Fig. 8. At 170 °C, the pullout torque is estimated to be 351 Nm which is 3.4 times higher than the rated system torque of 103.2 Nm. Therefore, the designed PMC is able withstand the higher temperatures while maintaining the sufficient pullout torque.

Lastly, in order to verify the effectiveness of PMC, the PM needs to be magnetized at all times during the operation. Demagnetization analysis is performed to evaluate the demagnetization ratio of both NdFeB and SmCo PMs of the optimized model. The SmCo PM is analyzed at a temperature of 200 °C while NdFeB is analyzed at 100 °C considering the ambient conditions. The maximum fluid temperature is estimated to be 170 °C. The analysis results show that SmCo PM is able to withstand a temperature of 200 °C without being demagnetized. The NdFeB PM shows a negligible demagnetization ratio of 0.17 % at few points as shown in Fig. 5. This shows that the optimized model is able to withstand high temperature conditions without getting demagnetized.

4. Experimental Results

The prototype PMC for 50 hp pump system was manu-

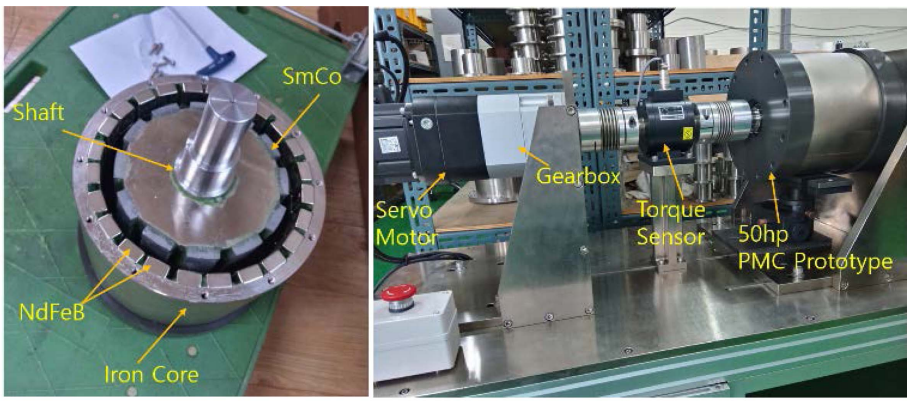

(a) (b)

Fig. 9. (Color online) Pullout torque measurement. (a) Prototype, (b) Test Setup.

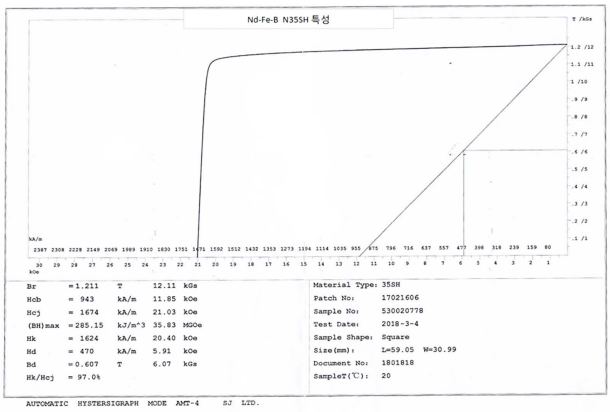

(a)

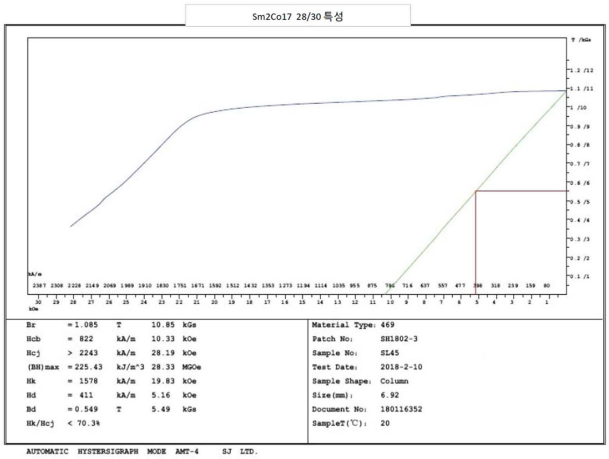

(b)

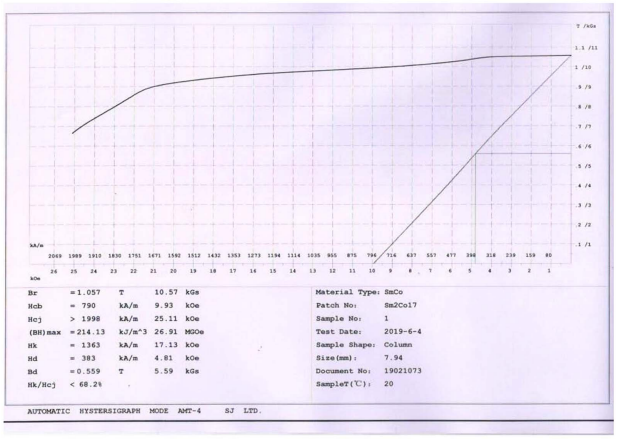

(c)

Fig. 10. (Color online) B-H Curves of the investigated PMs. (a) NdFeB with Br = 1.211 T, (b) SmCo with Br = 1.085 T, and (c) SmCo with Br = 1.057 T.

factured to test the pullout torque. The manufactured prototype and the test setup are shown in Fig. 9. The prototype was initially manufactured using SmCo PMs with a remanent flux density of 1.085 T. However, due to some reasons, these PMs were not fully magnetized. Later on, due to non-availability, these PMs were replaced with another grade SmCo PMs with a remanent flux density of 1.057 T. The simulated value of pullout torque was calculated as 408 Nm reducing from the previous value of 415 Nm. The B-H curves of the investigated PMs are shown in Fig. 10.

The test is conducted by connecting the inner part of the PMC with the drive motor. The outer part of the PMC is fixed to the casing and attached to the zig setup. The drive motor is rotated with a speed of 1 RPM and the pullout torque of the PMC is measured using a torque sensor. The torque sensor used in this experiment can measure torque up to 500 Nm. The drive motor can also provide torque of up to 500 Nm. The pullout torque measured using this configuration was found to be 392 Nm. The error between the measurement and FEM results is calculated as 3.7 % which can arise from various factors such as ambient temperature, servo-motor gearbox, FEM end effect limitations, installation and manufacturing limitations, etc. The pullout torque waveform comparison between FEM and test result is shown in Fig. 11. These pullout torque values are plotted over one pole-pitch or 180 electrical degrees. Table 2 shows the overall comparison of pullout torque and pullout torque per PM

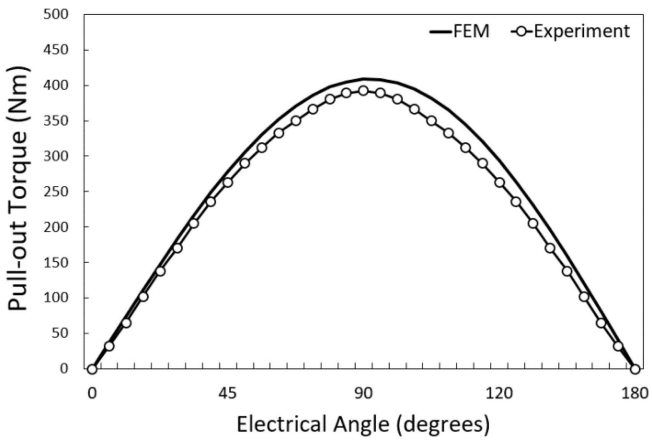

Fig. 11. Pullout torque comparison.

Table 2. Results Analysis.

Item	Unit	Optimized Model 3-D FEM	Optimized Model Experiment
Pullout Torque	Nm	408	392
Total PM Volume	dm^3	1.115	1.115
Pullout Torque / PM Volume	Nm/dm^3	365.9	351.3

volume of the FEM model and the prototype.

5. Conclusion

This paper presents a 12-pole permanent magnet coupling (PMC) for a 50 hp chemical pump. Due to relatively large airgap between the inner and outer part of the PMC, the PM shape is optimized to get maximum pullout torque for a given PM volume. The optimization process is based on the selection of linear and non-linear design parameters. The PM thickness and span are selected as design parameters for optimization due to their non-linear effects. Two models are initially investigated based on PM shape and eddy current analysis. The optimization is performed using Kriging method and genetic algorithm due to their effectiveness in analyzing non-linear parameters. 2-D FEM is performed for the design of experiments considering a constant stack length. After getting optimized design parameters, the stack length of the PMC is adjusted as a linear design parameter to get the required output pull-out torque while considering end effects as well. The optimized model is found to have highest pull-out torque per PM volume among the generated samples. The final model is verified using 3-D FEM and stack length is adjusted to get the desired pullout torque. Temperature and demagnetization analysis are also performed to verify the effectiveness of final model. Finally, a prototype is manufactured and the experimental results shows a good compliance with the FEM results.

Acknowledgments

This work was supported by the Korea Institute of Energy Technology Evaluation and Planning (KETEP) and the Ministry of Trade, Industry & Energy (MOTIE) of the Republic of Korea (No. 20172010106090).

References

[1] R. Ravaud, V. Lemarquand, and G. Lemarquand, IEEE Trans. Magn. **46**, 11 (2010).
[2] J. Charpentier and G. Lemarquand, IEEE Trans. Magn. **35**, 2 (1999).
[3] W. Wu, H. C. Lovatt, and J. B. Dunlop, IEEE Trans. Magn. **33**, 5 (1997).
[4] S. Högberg, B. B. Jensen, and F. B. Bendixen, IEEE Trans. Magn. **49**, 12 (2013).
[5] V. Lemarquand, J. Charpentier, and G. Lemarquand, IEEE Trans. Magn. **35**, 5 (1999).
[6] S. Rhyu, S. Khaliq, C. Baek, and Y. Ha, J. Magn. **25**, 64 (2020).